Electron and Spin Density Analysis of Spin-Projected Unrestricted Hartree-Fock Density Matrices of Radicals

Rainer Glaser* and Godwin Sik-Cheung Choy[1]

Department of Chemistry, University of Missouri, Columbia, Missouri 65211

Received: September 14, 1992

Methods have been developed for the electron and spin density analysis of unrestricted Hartree-Fock wave functions of radicals *without* and *with* the inclusion of annihilation of the largest spin contaminant via spin projection (PUHF). While UHF wave functions are not eigenfunctions of the $\langle S^2 \rangle$ operator, the spin projection method successfully annihilates the main component of the spin contamination. Electron and spin density functions determined at the UHF and PUHF levels are compared. Differences of topological and of integrated properties are discussed. Methyl and allyl radicals are discussed to illustrate the effects of spin annihilation. Representative series of simple binary radicals of first- and second-row atoms, of heteroatom-substituted methyl radicals, of a selected number of unsaturated systems, and of selected aza analogues of allyl radicals also are considered, and trends are discussed. It is found that the electron populations determined with the UHF and PUHF electron density functions differ only marginally but that the spin populations are greatly dependent on the method.

Introduction

Modern electron density analysis methods developed within the framework of the theory of atoms in molecules[2] are among the most useful tools for chemists to characterize and analyze bonding. The results of such an analysis not only allow for a better understanding of important chemical concepts, but they have lead to significant new findings; that is, such analyses go beyond a posteriori description in that they suggest new methods for the study of bonding and thus to advance our level of its understanding. The resonance concept, for example, has received significant attention recently[3] in light of electron density analyses, and the crucial importance of the atomic dipole moments for their interpretation has been stressed.[4] Unexpected new features in electron density distributions have been discovered.[5] Even such fundamental parameters as electronegativity[6] and bond dissociation energies,[7] processes such as charge transfers,[8] and concepts like the Hammond postulate[9] can be analyzed within this framework to reveal new insights into bonding.

Central to this theory is the idea of recovering the atom in the molecule based solely on the topological properties of the electron density distribution. The zero flux surfaces of the gradient of the electron density define the unambiguous partitioning of the three-dimensional electron density distribution into atomic basins. Numerical integration[10] of the appropriate electron density function within such basins yields integrated atomic properties that have a rigorous foundation in quantum mechanical theory. Numerical integration of the electron density itself results in atomic populations, and the integration of derived electron density functions yields integrated properties such as electric moments, kinetic energies, and many others. Here we will be primarily concerned with atom populations and atom first moments, important parameters for atom anisotropy, which are defined as

atom population: $$N = \int \rho(r)\, d\tau$$

first atom moment: $$\mu = -e \int r_\Omega \rho(r)\, d\tau$$

where the integrations are carried out over the entire basin $d\tau$ of atom Ω.[11] The topological electron density analysis technique differs fundamentally from other population analyses that employ basis set partitioning such as the Mulliken population analysis,[12] the Natural Population method,[13] or the SEN method.[14] The topological method has two major advantages.[15] First, it is the only method in which the partitioning of the molecular system into atomic regions is done in a rigorous manner based on the axioms of quantum mechanics, while all other methods involve further assumptions. Second, while all other methods provide only charges, the topological method provides additional information on the atomic properties such as atomic dipole moments and atom stabilities. While the application of the topological method to large systems was somewhat limited in the past by the substantial computer time requirements for the numerical integrations, recent developments by us[16] and others[17] have allowed for significantly more efficient integration procedures without any loss in accuracy.

Topological electronic density analysis has been widely applied at the restricted Hartree-Fock (RHF) level, and more recently, reports occur more frequently of electron density analysis with the inclusion of electron correlation effects via perturbation theory (e.g., second-order Møller-Plesset theory, MP2) as well as via variational theory (CISD).[18] Compared to our level of understanding of *closed*-shell systems, the study of *open*-shell systems is still in its infancy.[19] Much of the current lack of electronic structure analysis of radicals is due to the disadvantages associated with their Hartree-Fock level wave functions. Restricted open-shell Hartree-Fock theory (ROHF) does not account for spin polarization, and single excitations need to be considered to remedy this deficiency. The unrestricted formalism of Hartree-Fock theory (UHF) accounts for spin polarization as its allows for different spatial parts of the spin orbitals, but the UHF solutions are spin contaminated; that is, the wave functions are not eigenfunctions of the $\langle S^2 \rangle$ operator.

In this article, we report the results of a study of the electron density and the spin density analysis of radicals based on unrestricted wave functions *without* (UHF) and *with* (PUHF) the annihilation of spin contaminations through spin projection. Software was written and is described to accomplish this task. The comparative study of the effects of spin annihilation on the electron and on the spin density distributions and atom population is in the focus of the present study. Three types of open-shell systems were chosen to test and illustrate the methods and to search for general trends. To begin with, several simple binary radicals of first- and second-row atoms, $^\bullet XH_n$ (X = C, N, O and X = Si, P, S), were considered. As representatives of simple σ radicals, a series of heteroatom-substituted methyl radicals,

0022-3654/93/2097-3188$04.00/0

$^{\bullet}CH_2XH_n$ (X = F, O, N, C and Cl, S, P, Si), was considered, and a selected number of the unsaturated systems, $^{\bullet}CH_2X$ (X = CN, NO, CHO), were examined as well. Allyl radical and selected aza analogues were included in this study as prototypical π radicals.

Theoretical Background

An excellent review of UHF and spin-projected UHF theory by Rossky and Karplus is available,[20] and it allows us to be brief. For an open-shell N-electron system with the eigenvalue s_0 of the spin operator $\langle S_z \rangle$, the orbitals of a restricted open-shell Hartree–Fock (ROHF) wave function[21] are constructed from $0.5(N-2s_0)$ doubly occupied spatial orbitals and $2s_0$ singly occupied spatial orbitals. In the UHF formalism,[22] the constraint to double occupation is released, every electron can occupy an individual spin orbital with an independent spatial part, and the difference between the exchange interaction among α spin electrons and that among the β spin electrons in an open-shell system leads to the so-called spin polarization.[23] The difference between the α spin and the β spin spatial orbitals in the UHF wave functions leads to nonzero spin densities in the atomic regions, and the total spin in an atomic region is the "spin population".

For open-shell systems, the exact eigenfunctions are required to be eigenfunctions of both the total spin-angular momentum $\langle S^2 \rangle$ operator and of the z component of the S operator. While the ROHF method satisfies these conditions, the ROHF wave functions suffer from the neglect of spin polarization. On the other hand, the UHF solution accounts qualitatively for spin polarization, but it has a shortcoming in that the wave function is not an eigenfunction of the $\langle S^2 \rangle$ operator (but it is an eigenfunction[24] of $\langle S_z \rangle$). Because of this, UHF wave functions contain contaminations by higher spin multiplets.[25] Recently, spin-constrained unrestricted Hartree–Fock theory (SUHF) also has been introduced as a method for the determination of orbitals with different α and β spin while avoiding the spin contamination present in the UHF method.[26]

Löwdin showed that the dominant part of the spin contamination is due to contributions from the next higher spin state, and he devised a method to annihilate such spin contamination from the UHF wave function via a projection technique.[27,28] Partial[29] and full[30] annihilation of the major contamination due to the next higher spin state or complete annihilation of all contaminating spin states[31,32] has been examined subsequently.[33] More recently, Schlegel[34,35] demonstrated that spin projection of just the next higher spin state successfully removes most of the spin contamination from UHF wave functions.[36] Extension of the method to include perturbational effects of electron correlation also proved successful.[37,38] In the following, spin annihilation will refer to the removal of the major spin contamination due to the next higher spin state of the UHF wave function and the wave function thus produced will be referred to as the projected unrestricted Hartree–Fock (PUHF) wave function. UHF wave functions after complete annihilation of all spin contaminations will be denoted as CPUHF.

The eigenvalues of the $\langle S^2 \rangle$ operator of the UHF and of the PUHF wave functions of the radicals considered in this study are listed in Table I. As can be seen, the removal of the quartet contributions successfully removes the major part of the spin contamination.

Computational Implementation

For closed-shell systems, the determination of the topological and integrated atomic properties involves the following steps. An ab initio program such as Gaussian88 is used to determine the RHF wave function of the system. The wavefunction together with basis set and geometry data is read from the checkpoint file and written to a so-called WFN file in the appropriate format for subsequent density analysis. This task is accomplished with the program PSICHK.[39] The electron density analysis is accomplished in two steps with the programs SADDLE and PROAIM.[40] With the program SADDLE, the critical points in $\rho(x,y,z)$ are determined, that is, the points in Cartesian space at which the gradient of the density vanishes. With the critical point information, PROAIM performs the tasks of first defining the zero-flux surfaces and then determining atomic properties for each atom at a time by numerical integration.

TABLE I: Spin Contamination. Eigenvalues of the $\langle S^2 \rangle$ Operator[a]

radical	UHF	PUHF[b]	Δ[c]
CH_3	0.762	0.750	0.012
NH_2	0.758	0.750	0.008
OH	0.755	0.750	0.005
SiH_3 D_{3h}	0.767	0.750	0.017
SiH_3 C_{3v}	0.754	0.750	0.004
PH_2	0.763	0.750	0.013
SH	0.758	0.750	0.008
CH_2CH_3	0.762	0.750	0.012
CH_2NH_2	0.760	0.750	0.010
CH_2OH	0.759	0.750	0.009
CH_2F C_{2v}	0.763	0.750	0.013
CH_2F C_s	0.759	0.750	0.009
CH_2SiH_3	0.761	0.750	0.011
CH_2PH_2	0.765	0.750	0.015
CH_2SH	0.765	0.750	0.015
CH_2Cl C_{2v}	0.765	0.750	0.015
CH_2Cl C_s	0.764	0.750	0.014
CH_2CN	0.924	0.768	0.156
CH_2NO	1.010	0.761	0.249
CH_2CHO	0.936	0.755	0.181
CH_2CHCH_2	0.973	0.758	0.215
CH_2NCH_2	0.975	0.758	0.217
CH_2CHNH	0.976	0.757	0.219
CH_2NNH	0.998	0.758	0.240

[a] All values for the 6-31G* wave functions calculated with the UHF/6-31G* structures. [b] After annihilation of the next highest spin state (quartet). [c] Δ values give the difference between the eigenvalues before and after annihilation (UHF – PUHF).

In our work on the open-shell systems, modifications to all of these programs were made, and additional programs were written that allow for the electron and spin density analysis at the UHF and PUHF levels. This set of programs[41,42] consisting of the programs PSICHK PUHF, SADDLE PUHF, PROAIM PUHF, DENCUT, and DENADD is available from the authors. For UHF wave functions, the α and β electron density matrices are read from the checkpoint file with PSICHK PUHF and written to a WFN file that contains the α MOs and the β MOs in sequence. In the case of the PUHF calculations, appropriate nonstandard routes are used in running Gaussian88 to write out the PUHF density matrices for the α and β sets. With the programs DENCUT and PSICHK PUHF, the density matrices are reformated to obtain separate WFN files for the α and β densities. Program DENADD was written to construct WFN files for the total electron density and for the spin density functions. SADDLE PUHF is then employed to determine the topological properties of the total electron density function, and with PROAIM PUHF, the integrated properties for the two sets are determined.

The total electron density function is the sum of the α and β parts, and the spin density function is their difference.

electron density function: $\rho_t = \rho_\alpha + \rho_\beta$

spin density function: $\rho_t^S = \rho_\alpha - \rho_\beta$

For the analysis of the spin density function, two ways of partitioning might be pursued. One could either use the partitioning defined by the electron density function, or one might define a partitioning based solely on the phase changes in the ρ_t^S functions. The first partitioning method employs one and the same partitioning surface for the α, the β, and the total densities, this option is precedented,[19] and it is also the method that we

TABLE II: Electron and Spin Populations of Simple Binary Radicals

		PUHF				UHF			
		N_α	N_β	N^a	SP[b]	N_α	N_β	N	SP
					$\cdot CH_3$				
1	C	3.539	2.575	6.114	0.964	3.583	2.530	6.113	1.053
2	H	0.487	0.475	0.962	0.012	0.472	0.490	0.962	−0.018
					$\cdot NH_2$				
3	N	4.359	3.357	7.716	1.002	4.381	3.333	7.714	1.048
4	H	0.320	0.321	0.641	−0.001	0.309	0.333	0.642	−0.024
					$\cdot OH$				
5	O	4.796	3.791	8.587	1.005	4.804	3.782	8.586	1.022
6	H	0.204	0.209	0.413	−0.005	0.196	0.218	0.414	−0.022
					$\cdot SiH_3$ D_{3h}				
7	Si	6.242	5.542	11.784	0.700	6.279	5.509	11.788	0.770
8	H	0.914	0.816	1.730	0.098	0.902	0.828	1.730	0.074
					$\cdot SiH_3$ C_{3v}				
9	Si	6.276	5.524	11.800	0.752	6.287	5.513	11.800	0.774
10	H	0.906	0.824	1.730	0.082	0.902	0.828	1.730	0.074
					$\cdot PH_2$				
11	P	7.391	6.497	13.888	0.894	7.406	6.482	13.888	0.924
12	H	0.805	0.751	1.556	0.054	0.797	0.759	1.556	0.038
					$\cdot S H$				
13	S	8.503	7.513	16.016	0.990	8.511	7.506	16.017	1.005
14	H	0.497	0.487	0.984	0.010	0.489	0.494	0.983	−0.005

[a] Electron population N is the sum of the α and β populations: $N = N_\alpha + N_\beta$. [b] Spin population SP is the difference between the α and β populations: $SP = N_\alpha - N_\beta$.

have used throughout in the present work; that is, the electron populations were determined for the α and β parts of the density within the atomic basins of the total electron density to give N_α and N_β. The electron population then is the sum of N_α and N_β and the atom spin population, SP, is their difference.

electron population: $N = N_\alpha + N_\beta$

spin population: $SP = N_\alpha + N_\beta$

Results for Representative Series of Radicals

In Tables II–IV, the electron populations N_α and N_β, the total electron populations N, and the spin populations SP are given of all of the atoms of the simple binary radicals, of the substituted methyl radicals, and of allyl radical and its N analogues, respectively, as determined with the UHF and with the PUHF wave functions.

All wave functions were calculated with the UHF/6-31G* optimized structures.[43] Geometries were optimized with the appropriate symmetry constraints with Gaussian88, and the exact Hessian matrices were computed for each structure to assure its stationarity and to characterize each extremum as a minimum or as a transition-state structure via the number of negative eigenvalues.

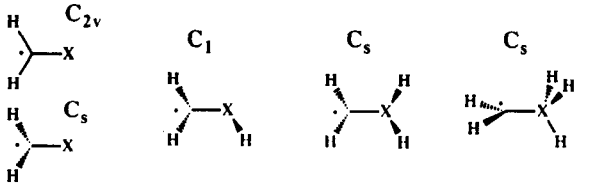

The XH_2 radicals (X = N, P) were calculated in C_{2v} symmetry. Methyl and silyl radicals both were optimized in D_{3h}. While D_{3h} CH_3 is the minimum, D_{3h} SiH_3 is the transition-state structure for inversion of the C_{3v} symmetric silyl radical. Both the D_{3h} and the C_{3v} silyl radical structures were studied. The substituted methyl radicals[44,45] were studied with the conformations and symmetries shown above. For the halogenated systems, both the C_s minima as well as the C_{2v} symmetric transition-state structures for inversion were considered. The hydroxy and thiomethyl radicals were computed in C_1 symmetry. Both heavy atoms are pyramidalized in the amino and phosphinomethyl radicals in the way shown, and they have overall C_s symmetry. The methyl and silyl-substituted methyl radicals are C_s symmetric with staggered conformations. In addition, the methyl radicals with an attached formyl, nitroso, or nitrile group were studied. These systems

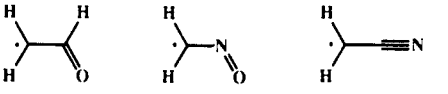

might equally well be regarded as heteroanalogues of the allyl radical. Their structures were optimized within the symmetry point groups shown and confirmed to be minima. Allyl radical,[46,47]

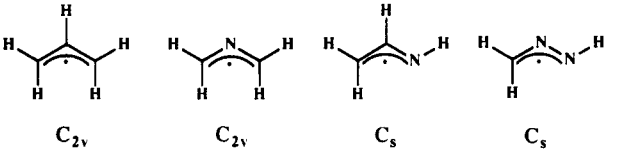

its 2-*N* and 1-*N* aza analogues, and its 1,2-*N*,*N* analogues[48] all were considered with the conformations and the symmetries[49] shown. For brevity, neither structural and energy data nor the results of the vibrational frequency analysis are given here. Many of these are available in the literature,[50] and the remaining data can be obtained from the authors.

Cross sections of the electron and spin densities were determined with our program Netz[51] and graphed with our PV-Wave programs. Computations were carried out on a network consisting of a Vaxstation3100, two VaxStation3520, two Silicon Graphics Personal Iris 4D/25 workstations, and on the IBM 4381 and 3090J mainframes of the Campus Computing Center and the attached FPS array processor.

Effects of Spin Annihilation on Topological Properties

In methyl radical, the unpaired electron occupies a C-p-AO. Because of this unpaired α spin at C, the paired α electrons in

TABLE III: Electron and Spin Populations of Substituted σ-Methyl Radicals

		PUHF				UHF			
		N_α	N_β	N	SP	N_α	N_β	N	SP
					$^{\bullet}CH_2CH_3$[b]				
15	C′	3.498	2.586	6.084	0.912	3.541	2.542	6.083	0.999
16	C	2.957	2.951	5.908	0.006	2.932	2.976	5.908	–0.044
17	H–(C)	0.525	0.488	1.013	0.037	0.532	0.481	1.013	0.051
18	H^S–(C)	0.511	0.502	1.013	0.009	0.513	0.500	1.013	0.013
19	H–(C′)	0.499	0.485	0.984	0.014	0.484	0.500	0.984	–0.016
					$^{\bullet}CH_2NH_2$				
20	C	3.158	2.362	5.520	0.796	3.188	2.333	5.521	0.855
21	N	4.221	4.065	8.286	0.156	4.222	4.068	8.290	0.154
22	H-(C)	0.503	0.483	0.986	0.020	0.491	0.496	0.987	–0.005
23	H–(N)	0.307	0.303	0.610	0.004	0.306	0.304	0.610	0.002
					$^{\bullet}CH_2OH$[c,d]				
24	C	3.109	2.289	5.398	0.820	3.139	2.260	5.399	0.879
25	O	4.696	4.557	9.253	0.139	4.693	4.560	9.253	0.133
26	H–(O)	0.200	0.200	0.400	0.000	0.199	0.201	0.400	–0.002
27	H^t	0.489	0.472	0.961	0.017	0.476	0.485	0.961	–0.009
28	H^c	0.505	0.482	0.987	0.023	0.493	0.493	0.986	0.000
					$^{\bullet}CH_2F$ C_{2v}				
29	C	3.140	2.269	5.409	0.871	3.178	2.230	5.408	0.948
30	H	0.464	0.457	0.921	0.007	0.447	0.474	0.921	–0.027
31	F	4.932	4.817	9.749	0.115	4.927	4.821	9.748	0.106
					$^{\bullet}CH_2F$ C_s				
32	C	3.108	2.251	5.359	0.857	3.138	2.221	5.359	0.917
33	H	0.482	0.464	0.946	0.018	0.469	0.478	0.947	–0.009
34	F	4.928	4.820	9.748	0.108	4.925	4.824	9.749	0.101
					$^{\bullet}CH_2SiH_3$[b]				
35	C	3.896	2.958	6.854	0.938	3.930	2.923	6.853	1.007
36	Si	5.507	5.506	11.013	0.001	5.499	5.514	11.013	–0.015
37	H–(Si)	0.878	0.855	1.733	0.023	0.880	0.852	1.732	0.028
38	H^S–(Si)	0.870	0.864	1.734	0.006	0.870	0.865	1.735	0.005
39	H–(C)	0.487	0.474	0.961	0.013	0.474	0.487	0.961	–0.013
					$^{\bullet}CH_2PH_2$				
40	C	3.836	2.946	6.782	0.890	3.872	2.908	6.780	0.964
41	P	6.616	6.565	13.181	0.051	6.606	6.581	13.187	0.025
42	H–(C)	0.482	0.470	0.952	0.012	0.468	0.484	0.952	–0.016
43	H–(P)	0.791	0.773	1.564	0.018	0.794	0.770	1.564	0.024
					$^{\bullet}CH_2SH$[c,d]				
44	C	3.535	2.677	6.212	0.858	3.578	2.633	6.211	0.945
45	S	8.011	7.897	15.908	0.114	7.995	7.913	15.908	0.082
46	H–(S)	0.506	0.501	1.007	0.005	0.506	0.502	1.008	0.004
47	H^t	0.472	0.462	0.934	0.010	0.458	0.477	0.935	–0.019
48	H^S	0.475	0.462	0.937	0.013	0.462	0.476	0.938	–0.014
					$^{\bullet}CH_2Cl$ C_{2v}				
49	C	3.415	2.521	5.936	0.894	3.462	2.473	5.935	0.989
50	H	0.456	0.448	0.907	0.011	0.440	0.465	0.905	–0.025
51	Cl	8.674	8.582	17.256	0.092	8.657	8.598	17.255	0.059
					$^{\bullet}CH_2Cl$ C_s				
52	C	3.401	2.514	5.915	0.887	3.446	2.470	5.916	0.976
53	H	0.461	0.451	0.912	0.010	0.447	0.465	0.912	–0.018
54	Cl	8.676	8.585	17.261	0.091	8.661	8.600	17.261	0.061
					$^{\bullet}CH_2CN$				
55	C	2.439	2.533	4.972	–0.094	2.287	2.700	4.987	–0.413
56	N	4.373	3.998	8.371	0.375	4.478	3.875	8.353	0.603
57	C′	3.283	2.571	5.854	0.712	3.360	2.496	5.856	0.864
58	H–(C′)	0.452	0.449	0.901	0.003	0.438	0.464	0.902	–0.026
					$^{\bullet}CH_2NO$				
59	N	3.942	3.586	7.528	0.356	4.036	3.483	7.519	0.553
60	O	4.559	3.808	8.367	0.751	4.610	3.753	8.363	0.857
61	C	2.564	2.684	5.248	–0.120	2.414	2.849	5.263	–0.435
62	H^t	0.466	0.464	0.930	0.002	0.466	0.463	0.929	0.003
63	H^c	0.474	0.462	0.936	0.012	0.478	0.457	0.935	0.021
					$^{\bullet}CH_2CHO$				
64	C	2.446	2.506	4.952	–0.060	2.329	2.641	4.970	–0.312
65	C′	3.367	2.702	6.069	0.665	3.451	2.622	6.073	0.829
66	O	4.748	4.369	9.117	0.379	4.802	4.293	9.095	0.509
67	H–(C)	0.494	0.492	0.986	0.002	0.495	0.491	0.986	0.004
68	H^c–(C′)	0.469	0.463	0.932	0.006	0.458	0.473	0.931	–0.015
69	H^t–(C′)	0.480	0.473	0.953	0.007	0.470	0.484	0.954	–0.014

[a] Compare legend to Table II. H^S: Symmetry-related H atoms in XH_3 group. H^t:H atom in the trans position. H^c:H atom in the cis position.

TABLE IV: Electron and Spin Population of the Allyl Radical and Selected Aza Analogues

		PUHF				UHF			
		N_α	N_β	N	SP	N_α	N_β	N	SP
					$^\bullet CH_2CHCH_2$				
70	H–(C)	0.498	0.494	0.992	0.004	0.501	0.492	0.993	0.009
71	C	2.933	3.043	5.976	–0.110	2.765	3.214	5.979	–0.449
72	C′	3.300	2.757	6.057	0.543	3.401	2.654	6.055	0.747
73	H^t–(C′)	0.493	0.488	0.981	0.005	0.484	0.497	0.981	–0.013
74	H^s–(C′)	0.491	0.486	0.977	0.005	0.482	0.496	0.978	–0.014
					$^\bullet CH_2NCH_2$				
75	N	4.250	4.274	8.524	–0.024	4.081	4.420	8.501	–0.339
76	C	2.898	2.394	5.292	0.504	3.001	2.302	5.303	0.699
77	H^t–(C)	0.482	0.477	0.959	0.005	0.471	0.488	0.959	–0.017
78	H^s–(C)	0.496	0.491	0.987	0.005	0.487	0.501	0.988	–0.014
					$^\bullet CH_2CHNH$				
79	C	2.570	2.671	5.241	–0.101	2.423	2.832	5.255	–0.409
80	N	4.337	3.830	8.167	0.507	4.411	3.740	8.151	0.671
81	H–(C)	0.501	0.498	0.999	0.003	0.503	0.496	0.999	0.007
82	H–(N)	0.316	0.319	0.635	–0.003	0.308	0.328	0.636	–0.020
83	C′	3.314	2.731	6.045	0.583	3.413	2.633	6.046	0.780
84	H^t–(C′)	0.474	0.469	0.943	0.005	0.464	0.479	0.943	–0.015
85	H^s–(C′)	0.488	0.482	0.970	0.006	0.478	0.492	0.970	–0.014
					$^\bullet CH_2NNH$				
86	N	3.886	3.957	7.843	–0.071	3.708	4.119	7.827	–0.411
87	N′	4.009	3.381	7.390	0.628	4.099	3.287	7.386	0.812
88	H–(N′)	0.311	0.315	0.626	–0.004	0.302	0.325	0.627	–0.023
89	C	2.853	2.412	5.265	0.441	2.968	2.316	5.284	0.652
90	H^s–(C)	0.471	0.468	0.939	0.003	0.462	0.477	0.939	–0.015
91	H^t–(C)	0.475	0.470	0.945	0.005	0.466	0.482	0.948	–0.016

[a] Compare legend to Table III.

the C–H bonds and close to this C tend to align themselves. The result is a larger α spin at C and a nonzero β spin at the hydrogens. This effect is the well-known spin polarization. Spin polarization in the allyl radical causes excess α spin on the terminal carbons and β spin accumulation at the central C, and all of the hydrogens carry the opposite spins relative to the C they are attached to. A contour plot of the spin density function (Figure 1) of methyl radical shows α spin in the C region and β spin in the H regions. The effect of the spin projection on the spin polarization is best seen by examination of the spin density difference function $\Delta\rho^S = \rho^S(\text{PUHF}) - \rho^S(\text{UHF})$. The function $\Delta\rho^S$ will be negative (dashed lines) at places where spin projection reduces the α spin, and it will be positive (solid lines) where it reduces the β spin. Contour and surface plots of the functions $\Delta\rho^S$ for methyl and allyl radical are shown in Figure 1. In both cases, we find that *spin annihilation reduces the spin polarization.* We will show (vide infra) that this is generally the case.

The significant effect of spin projection on the spin density distribution leaves the *electron density distribution essentially unaffected.* In Figure 2, surface plots of the electron density difference functions $\Delta\rho = \rho(\text{PUHF}) - \rho(\text{UHF})$ of methyl and allyl radicals are shown, respectively. Spin annihilation causes an increase of electron density in all bonding regions. Furthermore, spin annihilation is found to increase (decrease) the electron density in the proximity of these atoms with excess α (β) spin in UHF densities. Note, however, that all of the changes are *very small*: These features become apparent in contour plots only if very small contour level settings (between $\pm 10^{-4}$ e au^{-3}) are used.

The extremely small effects of the spin projection on the electron density distributions in methyl and allyl radicals *are typical and general* as is manifested quantitatively in the topological parameters of all other molecules as well. The topological properties are given as supplementary material. For example, all of the parameters derived from the UHF and PUHF densities are the same for $^\bullet CH_3$, and there are only slight differences in λ_2, λ_3, and ϵ for the allyl radical. These great similarities in the bond critical point data together with the marginally small effects on the $\Delta\rho$ functions strongly suggest that *the effects of spin projection on*

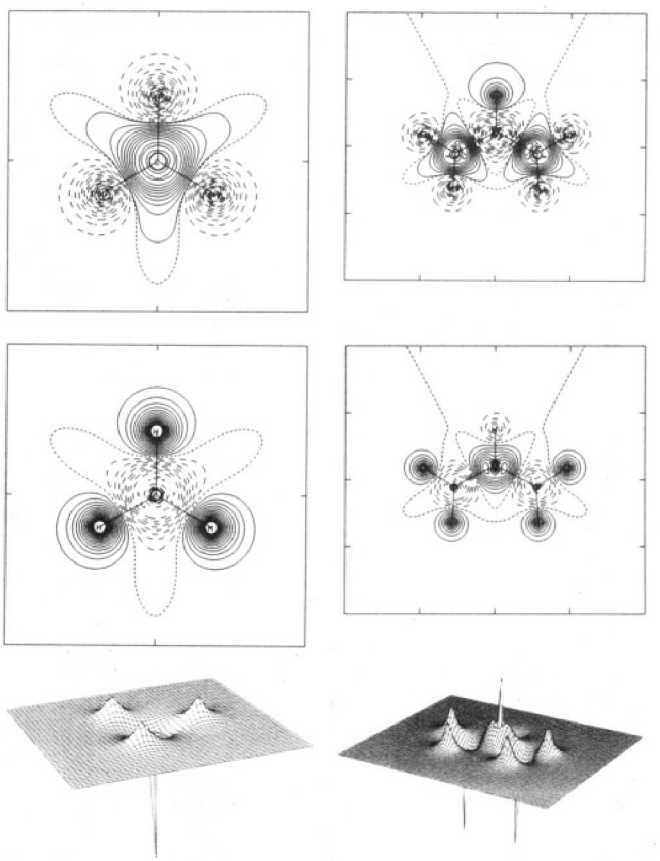

Figure 1. Contour plots of the spin density functions ρ^S(PUHF) of the methyl (left) and allyl radicals in the top row and respective spin density difference functions $\Delta\rho^S = \rho^S(\text{PUHF}) - \rho^S(\text{UHF})$ in the center row. Positive areas of the functions ρ^S and $\Delta\rho^S$ are contoured with solid lines, short dash indicates $\rho^S = 0$ and $\Delta\rho^S = 0$, and long dashed lines indicate contour negative regions of ρ^S and $\Delta\rho^S$. Contours for the ρ^S functions start at –0.01 e au^{-3} and increase with increments of 5×10^{-4}. For the difference function $\Delta\rho^S$ of the methyl (allyl) radical, contours start at –0.02 (–0.03) e au^{-3} with increments of 0.001 (0.0015). Surface plots of $\Delta\rho^S$ are shown at the bottom.

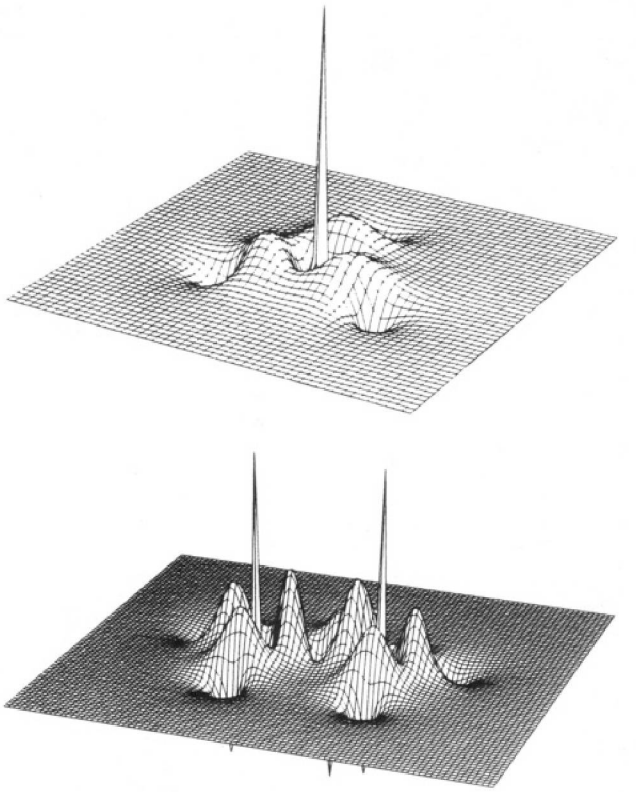

Figure 2. Surface plots of the electron density difference function $\Delta\rho = \rho(\text{PUHF}) - \rho(\text{UHF})$ of the methyl (top) and allyl radicals (logarithmic scale).

the electron density distribution—and thus also on the atomic basins—are marginal and virtually negligible.

Effects of Spin Projection on Integrated Properties

Integrations within the atomic basins defined by the zero-flux surfaces of the total electron density yield the populations associated with α and β spin components, N_α and N_β, the total electron population, $N = N_\alpha + N_\beta$, and the atom spin populations, $SP = N_\alpha - N_\beta$. These populations were determined at both of the levels UHF and PUHF, and the results are summarized in Tables II–IV.

Electron Populations. In Figure 3, the N(UHF) values are plotted vs the respective N(PUHF) values for all of the atoms. Linear regression results in a near-zero intercept, and the slope is very close to unity (eq 1). Similar correlations[52] were also found for the sets of all H atoms, of all C atoms, and all of the heteroatoms (eqs 2.1–2.3 in ref 52). All correlation coefficients differ less than 10^{-3} from unity.

$$N(\text{PUHF}) = 1.0002N(\text{UHF}) - 8.3564 \times 10^{-4} \qquad (1)$$

The total electron population differences $\Delta N = N(\text{PUHF}) - N(\text{UHF})$ are rather small in all cases; ΔN ranges from –0.018 to 0.023 (Tables II–IV). For atoms with excess α spin in the UHF densities, $N_\alpha(\text{UHF}) \geq N_\beta(\text{UHF})$, spin annihilation increases N_β and decreases N_α by about *the same amount* and vice versa. This finding holds for the σ as well as for the π radicals, and these results show that the integrated atom populations *are affected but marginally by spin projection.* Considering the representative scope of our selection of test molecules, our results suggest this significant finding to be true for doublets in general.

Atomic Anisotropies. The topological properties determined at UHF and PUHF levels show but marginal changes in all the *bonding regions*. The graphical analysis of the electron density difference functions $\Delta\rho$ goes beyond this finding in that it shows the (small) effect not only in the bonding regions but in *all regions* of the electron density distribution. The latter finds a first

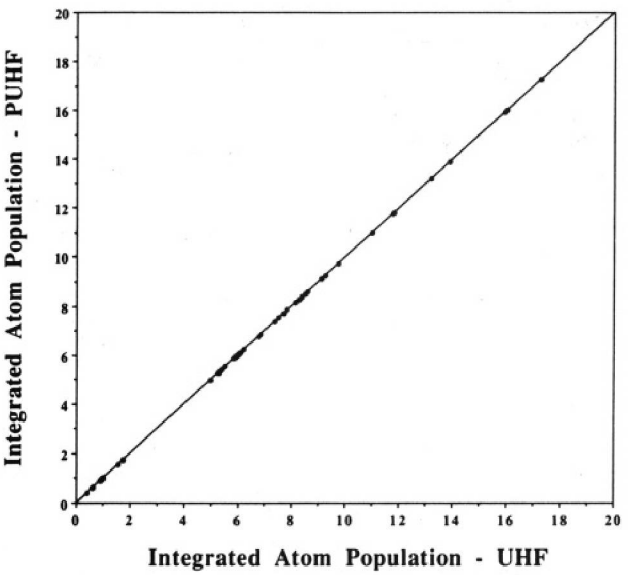

Figure 3. Integrated atom populations derived from UHF and PUHF density matrices linearly correlated. The regression includes all atoms of all systems studied.

manifestation in the small effects of projection on the electron populations. Nevertheless, the small ΔN values alone do not suffice to establish that the electron density *distribution* in the basins is not altered to any significant extent: Small ΔN values would occur in cases where significant redistribution of electron density *within* the basin occurs without significant charge transfer between the shape changes of the basins. While the graphical analysis of $\Delta\rho$ allows one to examine this question *qualitatively*, the atomic first moments μ allow *quantitative* conclusions because the first moment is a sensitive measure for the electron density distribution within the atomic basin.

We have determined the atomic first moments for all atoms of all the test molecules. The most pronounced effects of spin projection on atomic dipole moments were found for the allyl analogue π systems, and the results for this series are given in Table V. As can be seen, *neither the absolute magnitude nor the direction* of the atomic dipole moments is affected greatly by the projection operation. Positive and negative $\Delta\mu$ occur, and the absolute value of $\Delta\mu$ always is less than 0.10 au, smaller than 0.01 au in most cases, and 4×10^{-3} on average. The $\langle(\mu_A, A–B)$ values in Table V give the angles enclosed between the atomic dipole moment of atom A and the direction vector A → B as determined at the PUHF level. They are quite small (<0.1°) in general, but there are a few cases where large absolute μ values are associated with deviations of a few degrees (e.g., atoms 59 and 80).

Spin Populations. In marked contrast to the marginal effects of spin projection on the atom *electron* populations, *significant changes* of the atom *spin* populations are found. In Figure 4, the integrated atom spin populations SP(UHF) and SP(PUHF) are compared graphically. Positive SP values indicate excess α spin. In all cases, spin projection *decreases* the atom spin populations for atoms with excess α spin and it *increases* the atom spin populations for atoms with excess β spin.

$$\text{SP(PUHF)} < \text{SP(UHF)} \qquad \text{SP} > 0\ (\alpha \text{ spin})$$

$$\text{SP(PUHF)} > \text{SP(UHF)} \qquad \text{SP} < 0\ (\beta \text{ spin})$$

Implications. Amos examined atomic charges and spin densities for a small number of aromatic fused hydrocarbons and found that annihilation changes the charges hardly while the spin densities are changed significantly. In particular, he noted that the spin densities after annihilation were in better agreement with experiment.[53] In related studies, Harriman[54] concluded that

TABLE V: Atomic First Moments for the π Radicals[a,b]

A	atom	μ^{PUHF}	μ^{UHF}	$\Delta\mu$	$\angle(\mu_A,A-B)$	B	$\Delta(\mu\text{-dir})$
				$^{\bullet}CH_2CN$			
55	C	1.225	1.220	0.006	0.03	56	0.00
56	N	0.884	0.852	0.032	180.02	57	0.00
57	C′	0.439	0.440	−0.002	0.09	56	0.00
58	H−(C′)	0.135	0.135	0.000	0.43	57	0.04
				$^{\bullet}CH_2NO$			
59	N	1.205	1.176	0.028	16.43	60	0.99
60	O	0.228	0.230	−0.001	5.84	59	−0.19
61	C	0.906	0.910	−0.004	1.53	59	0.04
62	H^t	0.135	0.135	0.000	0.29	61	0.11
63	H^c	0.137	0.138	−0.001	0.76	61	−0.09
				$^{\bullet}CH_2CHO$			
64	C	0.880	0.879	0.001	118.59	65	0.42
65	C′	0.069	0.008	0.062	137.97	68	1.82
66	O	0.578	0.557	0.021	179.66	64	0.00
67	H−(C)	0.142	0.143	−0.001	2.92	64	0.03
68	H^c−(C′)	0.137	0.138	0.000	2.99	65	0.03
69	H^t−(C′)	0.139	0.139	0.000	1.04	65	−0.01
				$^{\bullet}CH_2CHCH_2$			
70	H−(C)	0.137	0.138	−0.001	0.01	71	0.00
71	C	0.054	0.063	−0.009	62.27	72	0.00
72	C′	0.068	0.080	−0.012	115.08	73	−1.27
73	H^t−(C′)	0.141	0.142	0.000	0.23	72	0.06
74	H^c−(C′)	0.140	0.140	0.000	0.22	72	−0.05
				$^{\bullet}CH_2NCH_2$			
75	N	0.266	0.244	0.022	120.48	76	0.00
76	C	0.831	0.833	−0.002	1.52	75	0.04
77	H^t−(C)	0.138	0.138	0.000	0.84	76	0.05
78	H^c−(C)	0.149	0.150	0.000	1.00	76	−0.05
				$^{\bullet}CH_2CHNH$			
79	C	0.759	0.756	0.002	3.20	80	−0.72
80	N	0.365	0.344	0.021	153.65	79	2.03
81	H−(C)	0.141	0.142	−0.001	0.18	79	0.00
82	H−(N)	0.191	0.191	0.000	0.19	80	−0.02
83	C′	0.094	0.105	−0.011	2.88	79	0.18
84	H^t−(C′)	0.138	0.139	0.000	3.21	83	0.05
85	H^c−(C′)	0.139	0.139	0.000	1.21	83	−0.03
				$^{\bullet}CH_2NNH$			
86	N	0.827	0.814	0.013	19.35	87	1.51
87	N′	0.684	0.692	−0.008	89.08	88	−0.11
88	H−(N′)	0.186	0.186	0.000	1.32	87	0.02
89	C	0.856	0.858	−0.002	0.80	86	0.04
90	H^c−(C)	0.142	0.143	0.000	2.41	89	0.07
91	H^t−(C)	0.135	0.135	−0.001	0.12	89	−0.05

[a] Atomic first moments μ^{UHF} and μ^{PUHF} determined by integration of the UHF and PUHF densities, respectively, in atomic units, and $\Delta\mu$ is their difference, $\Delta\mu = \mu^{PUHF} - \mu^{UHF}$. [b] The angles $\angle(\mu_A,A-B)$ between the atomic dipole of A and vector A → B are in degrees as determined with the PUHF densities, and $\Delta(\mu\text{-dir})$ values are the difference $\Delta(\mu\text{-dir}) = \angle(\mu_A,A-B)^{PUHF} - \angle(\mu_A,A-B)^{UHF}$.

"the spin density seems in general to be affected more than the charge density by projection". Subsequently, Nakatsuji et al.[55] showed in an elegant fashion that these conclusions can be derived from the knowledge that the charge density operator commutes with the annihilation operator, and they derived conditions that allow one to estimate the magnitude of these changes with an elaborate scheme.

Our results confirm and corroborate these prior theoretical analyses not only for *a broader scale of systems* but also with *quantitative estimates* of the effects of spin projection on electron and spin density distributions. Our results allow for the important conclusion that the electron density distributions of doublet radicals are affected by spin projection only to an insignificant extent. Hence, spin contamination of the UHF wave functions has but a marginal effect on the properties derived from the electron density function, and—for most practical purposes—*topological electron density analyses of UHF wave functions* without *projection of spin contaminations* yield reasonable results.

Effects of Spin Projection on Spin Populations

The spin population difference ΔSP, ΔSP = SP(PUHF) − SP(UHF), is a measure for the effect of the spin projection on the spin population. Figure 4 shows no general correlation between the ΔSP values and the magnitude of the atom spin population. For atoms with near-zero atom spin populations at the UHF level, the changes due to spin projection are negligible. The ΔSP values also are not correlated with the magnitude of the annihilated spin contamination in a simple and systematic fashion. In Figure 5, the ΔSP values are plotted vs the $\langle S^2\rangle$ eigenvalue differences $\Delta\langle S^2\rangle$, $\Delta\langle S^2\rangle = \langle S^2\rangle_{UHF} - \langle S^2\rangle_{PUHF}$, a measure of the annihilation of unwanted spin states, for all C atoms, all X atoms, and all H atoms. Spin population changes on the order of 0.1 may occur even for molecules with moderate-to-small spin contamination such as the σ radicals. For heavily spin-contaminated systems such as the π radicals, the ΔSP values become as large as 0.25–0.4. The ΔSP values for the H atoms are small thoughout ranging from −0.02 to 0.04, and the plot in Figure 5 shows that there is no correlation between ΔSP(H) and $\Delta\langle S^2\rangle$.

Simple Binary Radicals. In the XH_n radicals, the unpaired electron (with α spin) is located at the X atom, and on the top of Figure 6, the spin populations of the X atoms in these radicals are compared graphically, and a few trends are found. Two entries are made for $^{\bullet}SiH_3$; the entry on the left refers to the D_{3h} structure, and the other represents the pyramidal minimum structure. At the PUHF level, the SP(X) values increase with the group number

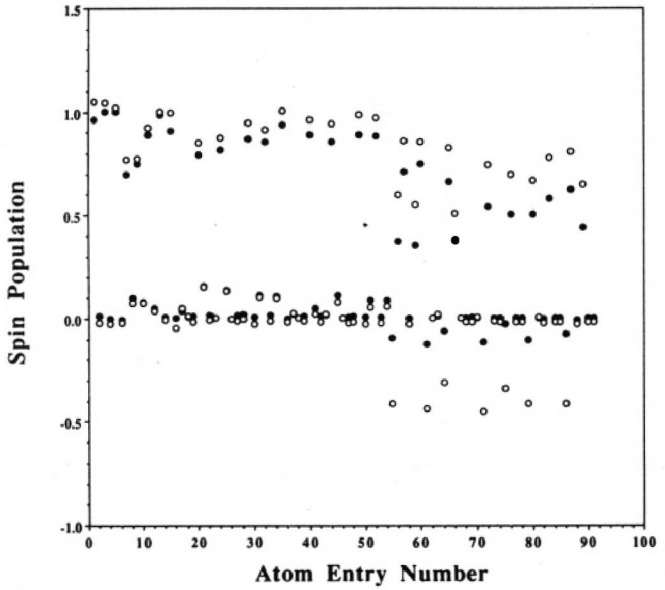

Figure 4. Spin populations SP(UHF) and SP(PUHF) graphed for all atoms. SP(PUHF) spin populations are marked by solid circles. Atom entry numbers refer to Tables II–IV.

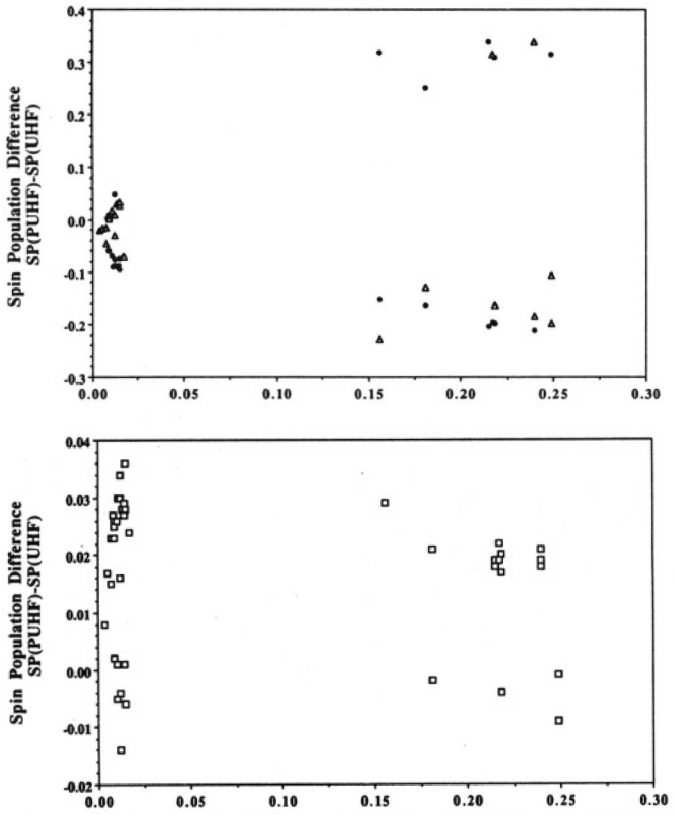

Figure 5. Spin population differences ΔS, ΔS = SP(PUHF) − SP(UHF), vs the reduction in the eigenvalues of the $\langle S^2 \rangle$ operator, $\langle S^2 \rangle_{UHF} - \langle S^2 \rangle_{PUHF}$, upon spin projection. The plot on top shows the data for all C atoms (black circles) and all heteroatoms (triangles), and the plot on the bottom shows the respective data for all hydrogen atoms.

within each row, and this increase is more pronounced for the second-row than for the first-row atoms. Thus, the projection technique always leads to a reduction of the spin polarization, and moreover, we find that this reduction of the spin population of X is inversely proportional to group number within a given row. Note that the spin populations determined at the UHF level also would indicate an increase in SP(X) as one moves to the right in the second row but just the opposite for the first-row systems.

Substituted Methyl Radicals. In the radicals CH_2XH_n, the X

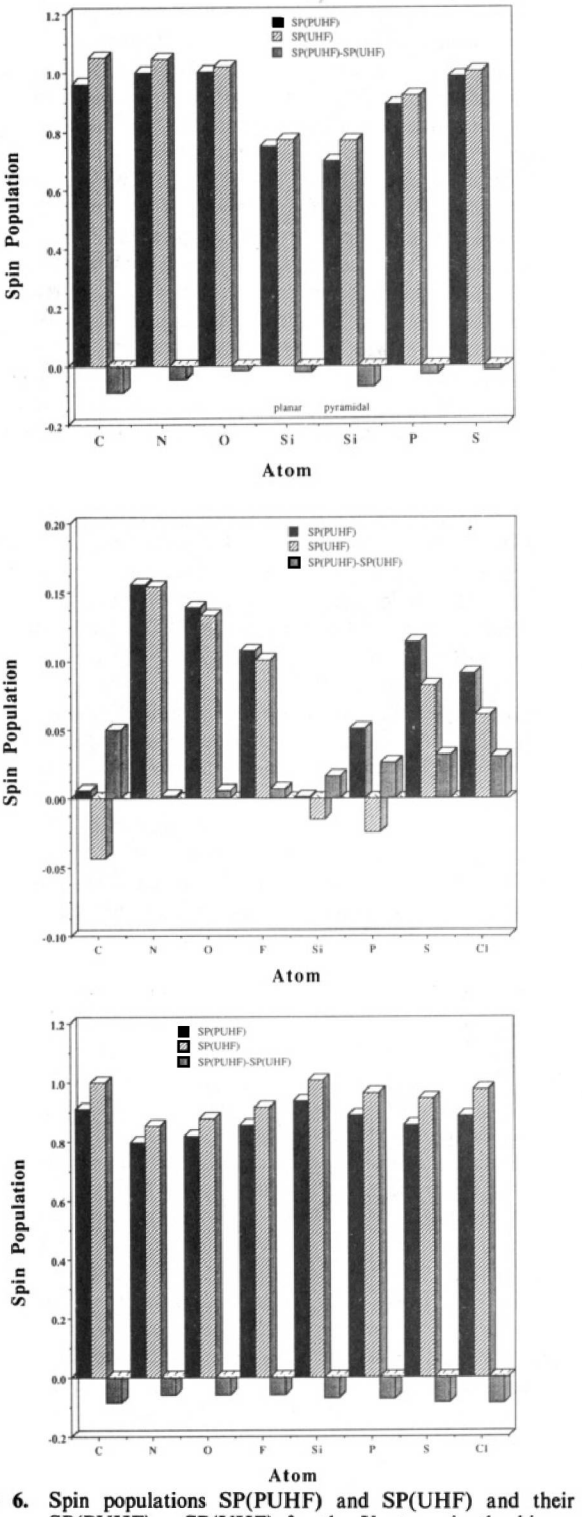

Figure 6. Spin populations SP(PUHF) and SP(UHF) and their differences SP(PUHF) − SP(UHF) for the X atoms in the binary compounds XH_n (top), the X atoms in H_2CXH_n (center), and for the C atoms in H_2CXH_n (bottom).

atoms no longer are the major spin carriers, but instead, most of the unpaired electron is located at the adjacent methyl carbons. Annihilation effects on X and the methyl C are compared graphically in Figure 6.

The spin populations calculated for the methyl carbons are affected qualitatively by the spin projection; the UHF and PUHF densities result in some cases in a reversal of the character of the spin at X. In the case of the ethyl radical, for example, the UHF method predicts a β spin population for the methyl group, whereas the methyl group is assigned an overall α spin after projection.

Intuitively, one might expect a rough correlation between the electron and the spin populations of the CH_2 groups in that the CH_2 groups with higher populations also have the higher spin populations, at least so long as only those test molecules without the possibility for delocalization in a π system[56] are considered. However, this expectation is not realized: The CH_2 group populations decrease with the electronegativity of X in each row as anticipated, but the spin populations of the methyl C and of the X atom show considerably more complex patterns (Figure 6). For each row, SP(X) goes through a maximum while SP(C) goes through a minimum as the group number of X increases, and these extrema occur later for the molecules with second-row substituents than with first-row substituents. Fluorine, for example, causes a higher CH_2 group electron deficiency compared to the amino group, but fluorine leaves the α spin excess at the CH_2 group higher nevertheless. The spin populations of the methyl C are always in excess of 0.8, and the SP(X) values are below 0.2.

Allyl Radicals and Analogues. The spin density distribution in the allyl radical shown in Figure 1 was discussed qualitatively above, and it is in excellent agreement with the experimental studies of its spin density distribution.[57] The terminal C atoms with SP(PUHF) = 0.54 have more than 0.5 α electron in excess, while the central C shows β spin density, SP(PUHF) = –0.11. Note the very significant reduction in the spin polarization upon projection of the first spin contaminant (Table IV), and significant changes of equal magnitude also are found for the spin populations of the heavy atoms in all of the heteroanalogues (Tables III and IV).

A detailed analysis of the electron and spin density distributions of the heteroanalogues of the allyl radical and its chemical implications will be presented in a separate paper. For brevity, here we mention only some results for the N analogues. Upon replacement of the terminal C atom by N, the N depletes the attached C atom of electron density but the spin density distribution is changed little. The spin density at the central C atom is rather similar compared to the allyl radical, and the large spin concentrations occur at the CH_2 carbon, SP(PUHF) = 0.583, and N, SP(PUHF) = 0.507. Replacement of the central CH group in the allyl radical by N merely changes the atomic charges as expected but again shows little effect on the spin distribution. In the radical CH_2NNH, we find similar effects, but in this case, the more electronegative terminal group NH also carries the higher spin population. Thus, allyl-radical-type spin delocalization persists upon C/N (and/or C/O) replacement, and it is accompanied by electron density shifts in the directions expected by atom electronegativities. Depending on the nature of the heterosubstitution, we may find anywhere between 40% and 60% of the unpaired electron at a given terminal atom, and this is in excellent agreement with the calculated bond lengths, which clearly imply significant radical delocalization through conjugation.

Fermi Contact and Spin Populations

By their definition, the Fermi contacts provide a measure for the spin density *in the vicinity of the nucleus*, and thus, Fermi contacts are intrinsically of a rather different nature than the integrated spin populations which provide a measure of the total spin density in the topologically defined atomic region. While the Fermi contact essentially reflects the spin density of the electrons near the nucleus, the spin population includes information about the core as well as the valence electrons. Accordingly, no general correlation between the Fermi contacts and the spin population is to be expected, and none occur.

In the case of the hydrogen atoms, however, one might expect that the spin density at the nucleus parallels the spin population, and the plots shown in Figure 7 do indeed show fairly good correlations between the spin populations and the Fermi contacts.

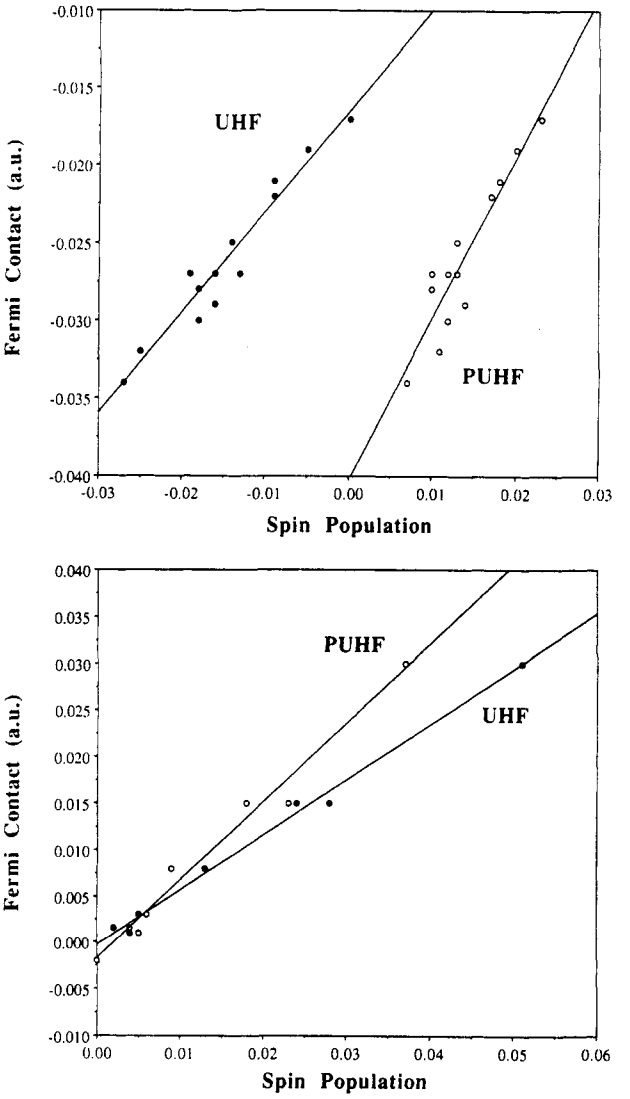

Figure 7. Correlation of Fermi contacts with spin populations. The Fermi contacts calculated at the UHF/6-31G* level are plotted vs the spin populations obtained at the UHF (solid circles) and PUHF (unfilled circles) levels. The plots on the top and bottom include all data for α- and β-hydrogens, respectively, in the substituted methyl radicals.

The data shown on top refer to all of the H atoms in the substituted methyl radicals that are connected to the methyl C atoms, the α-hydrogens, and the linear regression results in the equations

$$FC(\alpha\text{-H}) = 0.6478 \cdot SP(UHF) - 1.6582 \times 10^{-2} \quad (R^2 = 0.938) \quad (3.1)$$

$$FC(\alpha\text{-H}) = 1.0385 \cdot SP(PUHF) - 4.0379 \times 10^{-2} \quad (R^2 = 0.857) \quad (3.2)$$

The plot on the bottom shows the respective data for the β-hydrogens, that is, the H atoms attached to the heteroatom connected to the radical C, and the following equations best describe the correlations:

$$FC(\beta\text{-H}) = 0.5937 \cdot SP(UHF) - 3.2620 \times 10^{-4} \quad (R^2 = 0.993) \quad (4.1)$$

$$FC(\beta\text{-H}) = 0.8462 \cdot SP(PUHF) - 1.8394 \times 10^{-3} \quad (R^2 = 0.979) \quad (4.2)$$

The intercepts are close to zero in all cases, as expected, but the

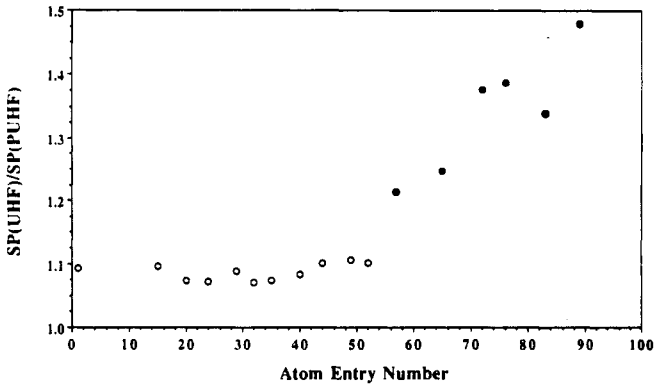

Figure 8. Ratio of spin populations SP(UHF)/SP(PUHF) for the C atoms in the σ radicals (unfilled circles) and in the π radicals, respectively.

slopes in eq 3 and 4 are significantly different and clearly indicate that even for the H atoms, this type of correlation does depend markedly on the bonding situation. The slopes are larger in both cases for the PUHF data which reflects the reduction in the spin polarization with spin projection (vide supra).

Spin Delocalization and Polarization

"Spin delocalization" and "spin polarization" have been used to classify "spin appearing" mechanisms that are due to singly occupied orbitals of the *best* restricted wave function or due to correlation between electron spins, respectively. Yonezawa et al.[58] proposed a scheme that allows for the separation of the spin density calculated with the UHF method without and with annihilation into components due to the spin polarization mechanism (SPM) and the spin delocalization mechanism (SDM). Yonezawa et al. have shown that the SPM contributions to the spin densities can be calculated with these equations:

$$SD(UHF)^{SPM} = s[1 + (2/s)][SD(UHF) - SD(PUHF)]$$

$$SD(PUHF)^{SPM} = s[1 + s^{-1}][SD(UHF) - SD(PUHF)]$$

$$SD(CPUHF)^{SPM} = s[SD(UHF) - SD(PUHF)]$$

The SDM contribution is the difference between the overall spin density SP and its SPM component; $SP^{SDM} = SP - SP^{SPM}$. The SPM contributions to the spin densities associated with the various stages of annihilation satisfy the relation

$$SD^{SPM}(UHF):SD^{SPM}(PUHF):SD^{SPM}(CPUHF) = (s + 2):(s + 1):s$$

and for our special case of doublet radicals, this equation becomes

$$SD^{SPM}(UHF):SD^{SPM}(PUHF):SD^{SPM}(CPUHF) = 3:2:1 \quad \textit{for } s = 1$$

This analytically derived relation motivated us to examine whether the ratio between the integrated spin populations determined at the UHF and PUHF levels might also approximate a constant. In Figure 8, we present graphically the spin population ratio SD(UHF)/SD(PUHF) for the C atoms in all of the σ radicals (unfilled circles) and in the π radicals. For the C atoms in the σ radicals, the ratio is found to be always about 1.1, while for the C atoms in the π systems, the ratios spanned a large range from 1.2 to 1.5. An interpretation of these ratios in terms of the spin appearing mechanism would be meaningful only if the spin densities calculated via the appropriate operator are related to the integrated SP values. Following the arguments presented in the discussion of the Fermi contacts, to expect such a relation might not be warranted, and the information in Figure 8 should be considered as empirical in nature.

Conclusion

Computer programs were written that allow for topological electron density and spin density analyses of densities of open-shell systems determined at the UHF and PUHF levels, that is, without and with removal of unwanted spin contaminations due to the next highest spin states via spin projection. The methods were tested, and topological and integrated properties were reported for representative series of simple binary radicals of first- and second-row atoms, $^{\bullet}XH_n$, for heteroatom-substituted methyl radicals, $^{\bullet}CH_2X$, for a selected number of the unsaturated systems, $^{\bullet}CH_2X$, and for selected aza analogues of the allyl radical.

Topological properties of bond critical points, graphical analyses of electron density difference functions $\Delta\rho = \rho(UHF) - \rho(PUHF)$, and quantitative determinations of atom populations and first moments at both levels show that the electron densities differ only *very* slightly. For studies of doublet radicals with focus on electron density distributions, we conclude that the analysis at the UHF level is appropriate and that spin contaminations have but a *very small* effect which is negligible for most types of analyses in theoretical organic studies. In marked contrast, we have found that spin projection affects the α and β spin components in greatly different fashions, and the spin populations determined at the UHF and PUHF levels thus differ *significantly*. Spin projection not only leads to substantial quantitative changes but it may result in qualitative changes and lead to reversal of trends.

In extensions of the presented study, the UHF and PUHF electron and spin density analyses will not only be compared to each other but also to the respective data determined at well-correlated levels of CASSCF theory. In a preliminary investigation, we have studied the binary radicals at levels up to the CASSCF[7,10] with structure optimizations at these levels. For structures and total energies, as well as for electron and spin populations, we have found that the spin annihilation method yields numbers that fall between the UHF and CASSCF data. Thus, these preliminary results strongly suggest not only that the spin projection remedies the spin contamination problem but that this modification does produce a density that is actually "improved" in that the changes associated with the spin projection converge toward the highest level theoretical results.

The analysis of Nakatsuji et al. suggests that the weight of the lowest contaminating spin function included in the UHF wave function decreases with increasing spin multiplicity. Hence, extrapolation of our results for the doublets to radicals with higher multiplicities might not be straightforward. In the latter case, complete annihilation of spin contaminations might be required, and studies are now in progress to clarify this question.

Acknowledgment is made to the donors of the Petroleum Research Fund, administered by the American Chemical Society, for support of this research. R.G. gratefully acknowledges financial support by a UMC Summer Research Fellowship and by a grant from the MU Research Board, and he thanks MURR for funds to attend the Gordon Research Conference on "Electron Density Distribution and Chemical Bonding". We thank the Campus Computing Center for generous allowance of computer time.

Supplementary Material Available: Three tables listing bond critical point information for the UHF and PUHF densities of the three series of molecules, with location of each bond critical point characterized via the absolute parameters r_A and r_B and the relative parameter F, via the value of the electron density at that point ρ, via the principal curvatures λ_i, and via the bond ellipticity ϵ (5 pages). Ordering information is given on any current masthead page.

References and Notes

(1) (a) Part of the projected Ph.D dissertation of G. S.-C. Choy. (b) Presented in part at the Midwest Meeting of the American Chemical Society,

Omaha, NE, Nov 1991. (c) Presented at the Gordon Conference on "Electron Density and Chemical Bonding", Plymouth, NH, July 1992.

(2) (a) Bader, R. F. W. *Atoms in Molecules—A Quantum Theory*; Clarendon Press: Oxford, U.K., 1990. (b) Bader, R. F. W. *Chem. Rev.* 1991, *91*, 893. (c) Bader, R. F. W. *Acc. Chem. Res.* 1985, *18*, 9.

(3) (a) Wiberg, K. B.; Laidig, K. E. *J. Am. Chem. Soc.* 1987, *109*, 5935. (b) Siggel, M. R. F.; Streitwieser, A.; Thomas, T. D. *J. Am. Chem. Soc.* 1988, *110*, 8022. (c) Wiberg, K. B.; Glaser, R. *J. Am. Chem. Soc.* 1992, *114*, 841 and preceding paper.

(4) (a) Glaser, R. *J. Comput. Chem.* 1990, *11*, 663. (b) Glaser, R.; Horan, C. J.; Nelson, E.; Hall, K. *J. Org. Chem.* 1992, *57*, 215. (c) Glaser, R.; Choy, G. S.-C. *J. Am. Chem. Soc.*, in press.

(5) (a) Cao, W.; Gatti, C.; McDougall, P. J.; Bader, R. F. W. *Chem. Phys. Lett.* 1987, *141*, 380. (b) Glaser, R.; Waldron, R. F.; Wiberg, K. B. *J. Phys. Chem.* 1990, *94*, 7357. (c) Cioslowski, J. *J. Phys. Chem.* 1990, *94*, 5496.

(6) Boyd, R. J.; Boyd, S. L. *J. Am. Chem. Soc.* 1992, *114*, 1652.

(7) Glaser, R.; Choy, G. S.-C.; Horan, C. J. *J. Org. Chem.* 1992, *57*, 995.

(8) Glaser, R.; Horan, C. J.; Choy, G. S.-C. *J. Phys. Chem.* 1992, *96*, 3689.

(9) Cioslowski, J. *J. Am. Chem. Soc.* 1991, *113*, 6756.

(10) Biegler-König, F. W.; Bader, R. F. W.; Tang, T. H. *J. Comput. Chem.* 1982, *3*, 317.

(11) See ref 2a, p 182ff.

(12) Mulliken, R. S. *J. Chem. Phys.* 1955, *23*, 1833, 1841, 2338, 2343.

(13) Reed, A. E.; Weinstock, R. B.; Weinhold, F. *J. Chem. Phys.* 1985, *83*, 735.

(14) (a) Davidson, R. E. *J. Chem. Phys.* 1967, *46*, 3320. (b) Ehrhardt, C.; Ahlrichs, R. *Theoret. Chim. Acta* 1985, *68*, 231.

(15) For a comparison, see for example: Glaser, R. *J. Comput. Chem.* 1989, *10*, 118.

(16) Glaser, R.; Harris, B. L. *THEOCHEM* 1992, *255*, 45.

(17) Cioslowski, J. *Chem. Phys. Lett.* 1992, *194*, 73.

(18) For studies of correlation effects on electron density distributions, see: Wiberg, K. B.; Hadad, C. M.; LePage, T. J.; Breneman, C. M.; Frisch, M. J. *J. Phys. Chem.* 1992, *96*, 671 and references cited there.

(19) (a) Bader, R. F. W.; Gangi, R. A. *J. Am. Chem. Soc.* 1971, *93*, 1831. (b) Bader, R. F. W.; Stephens, M. E.; Gangi, R. A. *Can. J. Chem.* 1977, *55*, 2755. (c) MacDougall, P.; Bader, R. F. W. *Can. J. Chem.* 1986, *64*, 1496.

(20) Karplus, M.; Rossky, P. J. *J. Chem. Phys.* 1980, *73*, 6196.

(21) McWeeny, R.; Dierksen, G. *J. Chem. Phys.* 1968, *49*, 4852.

(22) Pople, J. A.; Nesbet, R. K. *J. Chem. Phys.* 1954, *22*, 571.

(23) Nakatsuji, H.; Kato, H.; Yonezawa; T. *J. Chem. Phys.* 1969, *51*, 3175.

(24) Musher, J. I. *Chem. Phys. Lett.* 1970, *7*, 397 and references cited therein.

(25) See for example: Löwdin, P. O. *Quantum Theory of Atoms, Molecules, and the Solid State*; Academic Press: New York, 1966, p 601.

(26) (a) Amos, R. D.; Andrews, J. S.; Handy, N. C.; Knowles, P. J. *Chem. Phys. Lett.* 1991, *185*, 256–264. (b) Kowles, P. J.; Andrews, J. S.; Amos, R. D.; Handy, N. C.; Pople, J. A. *Chem. Phys. Lett.* 1991, *186*, 130–136.

(27) Löwdin, P. O. *Phys. Rev.* 1955, *97*, 1509.

(28) See also: Marshall, W. *Proc. Phys. Soc. London* 1961, *78*, 113.

(29) Amos, T.; Hall, G. G. *Proc. R. Soc. London, Ser. A* 1961, *263*, 483.

(30) Amos, T.; Snyder, L. C. *J. Chem. Phys.* 1964, *41*, 1773.

(31) Harriman, J. E. *J. Chem. Phys.* 1964, *40*, 2827.

(32) Phillips, D. H.; Schug, J. G. *J. Chem. Phys.* 1974, *61*, 1031.

(33) For a comparison of spin densities of hydrocarbons determined at all of these levels, see: (a) Chipman, D. M. *J. Chem. Phys.* 1979, *71*, 761. And for related studies, see also: (b) Chipman, D. M. *J. Chem. Phys.* 1983, *78*, 4785. (c) Chipman, D. M. *J. Phys. Chem.* 1992, *96*, 3294.

(34) Schlegel, B. *J. Chem. Phys.* 1986, *84*, 4530.

(35) Gonzalez, C.; Sosa, C.; Schlegel, H. B. *J. Phys. Chem.* 1989, *93*, 2435.

(36) For a discussion of the single annihilation equations of spin-projected UHF energies in a dissociating systems, see also: Koga, N.; Yamashita, K.; Morokuma, K. *Chem. Phys. Lett.* 1991, *184*, 359.

(37) (a) Sosa, C.; Schlegel, H. B. *Int. J. Quant. Chem.* 1986, *26*, 1002. (b) Sosa, C.; Schlegel, H. B. *J. Am. Chem. Soc.* 1987, *109*, 7007. (c) Sosa, C.; Schlegel, H. B. *J. Am. Chem. Soc.* 1987, *109*, 4193. (d) Sosa, C.; Schlegel, H. B. *Int. J. Quant. Chem.* 1987, *21*, 267. (e) Schlegel, H. B. *J. Phys. Chem.* 1988, *92*, 3075. (f) McDouall, J. J. W.; Schlegel, H. B. *J. Chem. Phys.* 1989, *90*, 2363. (g) Schlegel, H. B.; Soza, C. *Chem. Phys. Lett.* 1988, *145*, 329. (h) Gonzalez, C.; McDouall, J. J. W.; Schlegel, H. B. *J. Phys. Chem.* 1990, *94*, 7467. (i) Gonzalez, C.; Theisen, J.; Schlegel, H. B.; Hase, W. L.; Kaiser, E. W. *J. Phys. Chem.* 1992, *96*, 1767.

(38) (a) Murray, C. W.; Handy, N. C. *J. Chem. Phys.* 1992, *97*, 6509. (b) Knowles, P. J.; Handy, N. C. *J. Chem. Phys.* 1988, *88*, 6991. (c) Knowles, P. J.; Handy, N. C. *J. Phys. Chem.* 1988, *92*, 3097.

(39) (a) PSICHK: Lepage, T. J. Department of Chemistry, Yale University, 1988. (b) IBM version PSICHK IBM: Harris, B. Department of Chemistry, University of Missouri—Columbia, 1991.

(40) SADDLE and PROAIM: (a) Biegler-König, F. W.; Bader, R. F. W.; Tang, T. H. *J. Comput. Chem.* 1982, *3*, 317. (b) SADDLE and PROAIM were ported to IBM 4381 by G. S.-C. Choy and to the Silicon Graphics Personal Iris by R. Glaser.

(41) PSICHK PUHF, SADDLE PUHF, and PROAIM PUHF by G. S.-C. Choy and R. Glaser, University of Missouri—Columbia, 1990.

(42) DENCUT and DENADD by G. S.-C. Choy and R. Glaser, University of Missouri—Columbia, 1990.

(43) (a) Hehre, W. J.; Ditchfield, R.; Pople, J. A. *J. Chem. Phys.* 1972, *56*, 2257. (b) Hariharan, P. C.; Pople, J. A. *Theoret. Chim. Acta* 1973, *28*, 213. (c) Binkley, J. S.; Gordon, M. S.; DeFress, D. J.; Pople, J. A. *J. Chem. Phys.* 1982, *77*, 3654.

(44) For 4-31G studies of substituted methyl radicals, see for example: Pasto, D. J.; Krasnansky, R.; Zercher, C. *J. Org. Chem.* 1987, *52*, 3062.

(45) UHF/6-311++G** of CH_2X, X = SH, OH, and NH_2, were reported recently (Downard, K. M.; Sheldon, J. C.; Bowie, J. H.; Lewsi, D. E.; Hayes, R. N. *J. Am. Chem. Soc.* 1989, *111*, 8112), and the structures agree very well with the UHF/6-31G* structures used here.

(46) For a study of allyl cation, radical, and anion at SCF/6-31G* study, see: Schleyer, P. v. R. *J. Am. Chem. Soc.* 1985, *107*, 4793.

(47) For theoretical studies of allyl radical, see for example: (a) Peyerimhoff, S. D.; Buenker, R. J. *J. Chem. Phys.* 1969, *51*, 2528. (b) Levin, G.; Goddard, W. A., III. *J. Am. Chem. Soc.* 1975, *97*, 1649. (c) Takada, T.; Dupuis, M. *J. Am. Chem. Soc.* 1983, *105*, 1713. (d) Ha, T.-K.; Bauman, H.; Oth, J. F. M. *J. Chem. Phys.* 1986, *85*, 1438.

(48) McKee, M. L. *J. Am. Chem. Soc.* 1990, *112*, 7957.

(49) For discussions of the symmetry dilemma in allyl radical, see for example: (a) McKelvey, J.; Hehre, W. J. *Molec. Phys.* 1973, *25*, 983. (b) McKelvey, J. M.; Berthier, G. *Chem. Phys. Lett.* 1976, *41*, 476. (c) Paldus, J.; Veillard, A. *Chem. Phys. Lett.* 1977, *50*, 6. (d) Kikuchi, O. *Chem. Phys. Lett.* 1980, *72*, 487. (e) See also the paper by Musher (1970) referenced above.

(50) Hehre, W. J.; Radom, L.; Schleyer, P. v. R.; Pople, J. A. *Ab. Initio Molecular Orbital Theory*; John Wiley & Sons: New York, 1986.

(51) Netz and Dipoles by Glaser, R. University of Missouri—Columbia, 1990.

(52) Equation 2.1 for all H: $N(\mathrm{PUHF}) = 1.0004N(\mathrm{UHF}) - 6.4107 \times 10^{-4}$. Equation 2.2 for all C: $N(\mathrm{PUHF}) = 1.0101N(\mathrm{UHF}) - 6.2236 \times 10^{-3}$. Equation 2.3 for all X: $N(\mathrm{PUHF}) = 0.9988N(\mathrm{UHF}) - 1.7288 \times 10^{-2}$.

(53) Amos, A. T. *Molec. Phys.* 1962, *5*, 91.

(54) Harriman, J. E. (1964) cited above.

(55) Nakatsuji, H.; Kato, H.; Yonezawa, T. *J. Chem. Phys.* 1969, *51*, 3175.

(56) Without consideration of the NO-, CN-, and CHO-substituted systems.

(57) (a) Heller, C.; Cole, T. *J. Chem. Phys.* 1961, *37*, 243. (b) Fessenden, R. W.; Schuler, R. H. *J. Phys. Chem.* 1969, *39*, 2147. (c) Smart, B. E.; Krusic, P. J.; Meakin, P.; Bingham, R. C. *J. Am. Chem. Soc.* 1974, *96*, 7382. (d) Sustmann, R.; Trill, H. *J. Am. Chem. Soc.* 1974, *96*, 4343. (e) Korth, H.-G.; Trill, H.; Sustmann, R. *J. Am. Chem. Soc.* 1981, *103*, 4483.

(58) (a) Yonezawa, T.; Nakatsuji, H.; Kawamura, T.; Kato, H. *J. Chem. Phys.* 1969, *51*, 669. (b) Yonezawa, T.; Nakatsuji, H.; Kawamura, T.; Kato, H. *Chem. Phys. Lett.* 1968, *2*, 454. (c) Nakatsuji et al. (1969) cited above.